



**HAL**  
open science

## Intermittency and scale-dependent statistics in fully developed turbulence

Katsunori Yoshimatsu, Naoya Okamoto, Kai Schneider, Yukio Kaneda, Marie Farge

► **To cite this version:**

Katsunori Yoshimatsu, Naoya Okamoto, Kai Schneider, Yukio Kaneda, Marie Farge. Intermittency and scale-dependent statistics in fully developed turbulence. *Physical Review E*, 2009, 79, 10.1103/PhysRevE.79.026303 . hal-04113783

**HAL Id: hal-04113783**

**<https://hal.science/hal-04113783v1>**

Submitted on 2 Jun 2023

**HAL** is a multi-disciplinary open access archive for the deposit and dissemination of scientific research documents, whether they are published or not. The documents may come from teaching and research institutions in France or abroad, or from public or private research centers.

L'archive ouverte pluridisciplinaire **HAL**, est destinée au dépôt et à la diffusion de documents scientifiques de niveau recherche, publiés ou non, émanant des établissements d'enseignement et de recherche français ou étrangers, des laboratoires publics ou privés.

# Intermittency and scale-dependent statistics in fully developed turbulence

Katsunori Yoshimatsu,<sup>1</sup> Naoya Okamoto,<sup>1</sup> Kai Schneider,<sup>2</sup> Yukio Kaneda,<sup>1</sup> and Marie Farge<sup>3</sup>  
<sup>1</sup>*Department of Computational Science and Engineering, Nagoya University, Nagoya 464-8603, Japan*  
<sup>2</sup>*M2P2-CNRS and Universités d'Aix-Marseille, 38 rue F. Joliot-Curie, 13451 Marseille Cedex 20, France*  
<sup>3</sup>*LMD-IPSL-CNRS, Ecole Normale Supérieure, 24 rue Lhomond, 75231 Paris Cedex 05, France*  
 (Received 11 July 2008; published 5 February 2009)

Fully developed homogeneous isotropic turbulent fields, computed by direct numerical simulation, are compared to divergence-free random fields having the same energy spectrum and either the same helicity spectrum as that of the turbulent data, or vanishing helicity. We show that the scale-dependent velocity flatness quantifies the spatial variability of the energy spectrum. The flatness exhibits a substantial increase at small scales for the turbulent field, but remains constant for the random fields. A diagnostic, the scale-dependent helicity, is proposed to quantify the geometrical statistics of the flow, which shows that only the turbulent flow is intermittent. Finally, statistical scale-dependent analyses of both Eulerian and Lagrangian accelerations confirm the inherently different dynamics of turbulent and random flows.

DOI: 10.1103/PhysRevE.79.026303

PACS number(s): 47.27.E-, 47.27.Gs

## I. INTRODUCTION

Fully developed turbulence is characterized by its wide range of dynamically active scales. Isolated bursts of small scale activity are observed in many quantities, such as vorticity or energy dissipation, and lead to an inhomogeneous distribution of the small scale activity in space and time, a property which is generally called flow intermittency. This behavior is typically reflected by an anomalous scaling, e.g., the power law exponents  $\zeta(p)$  of the  $p$ th order velocity structure functions are below Kolmogorov's prediction  $p/3$  for increasing  $p$  [1]. As first suggested by Batchelor and Townsend [2], intermittency is attributed to the self-organization of the flow and the emergence of coherent structures. However, a complete understanding of the origins of intermittency and its quantification is still missing. In the present paper, we address the question: Is the classical description in terms of energy spectrum and the probability distribution functions (PDFs) of velocity increments sufficient to characterize intermittency? We propose different scale-dependent statistics based on the wavelet decomposition and apply them to several turbulent and random flow fields. In particular, we introduce a diagnostic, the scale-dependent relative helicity, with which we analyze geometrical statistics at different scales. Further insight into the dynamical processes is gained by considering scale-dependent higher order statistics of both Eulerian and Lagrangian accelerations.

## II. METHODOLOGY

The three-dimensional flow fields we study here are three different divergence-free velocity fields  $\mathbf{u}$  having the same energy spectrum  $E(k)$ , defined as  $E(k) = \int_{k=|k|} |\hat{\mathbf{u}}(\mathbf{k})|^2 d\mathbf{k}/2$ , where  $\hat{\mathbf{u}}$  is the Fourier transform of  $\mathbf{u}$ . The first field (a) is the velocity at a given instant of a statistically stationary homogeneous isotropic turbulent flow. It has been computed by direct numerical simulation (DNS) at resolution  $N=2048^3$ , which corresponds to a Taylor microscale Reynolds number  $R_\lambda=732$  and presents an energy spectrum  $E(k) \propto k^{-5/3}$ , as

shown in Fig. 1 [3–6]. In addition, we generate two synthetic divergence-free Gaussian isotropic random fields, (b) and (c). Field (b) is obtained by decomposing the Fourier coefficients of the DNS velocity field  $\mathbf{u}$  into helical waves  $\mathbf{h}^\pm$  (see, for instance, [7]),  $\hat{\mathbf{u}}(\mathbf{k}) = \hat{a}^+(\mathbf{k})\mathbf{h}^+(\mathbf{k}) + \hat{a}^-(\mathbf{k})\mathbf{h}^-(\mathbf{k})$ , with  $\mathbf{h}^\pm(\mathbf{k}) \cdot \mathbf{k} = 0$ , and randomizing the phases of the coefficients  $\hat{a}^\pm$ . This method thus preserves energy and helicity spectra. Field (c) corresponds to a divergence-free Gaussian random field with vanishing helicity, obtained by imposing  $\hat{a}^+(\mathbf{k}) = \hat{a}^-(\mathbf{k})$ , which has the same energy spectrum  $E(k)$  as the DNS field. A departure from the random fields may provide a basic measure of the space and scale non-Gaussian characteristics and the flow intermittency (see, e.g., [8–12]). A comparison of turbulent and random fields having the same energy spectrum was presented in [9] showing that no vortical structures are present in the latter.

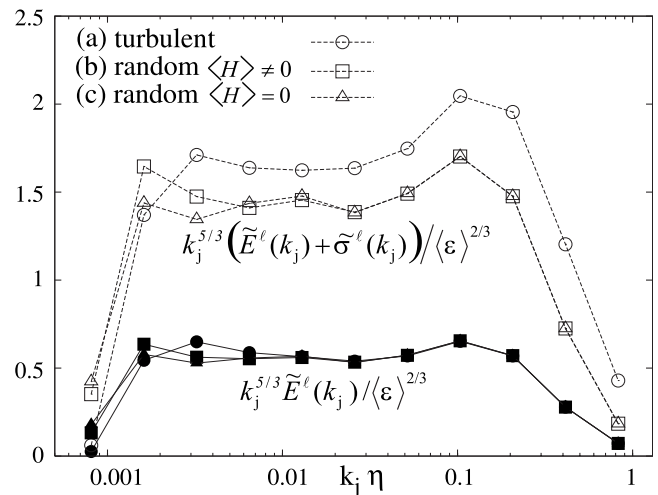


FIG. 1. Solid lines: Compensated wavelet spectrum  $k_j^{5/3} \tilde{E}^\ell(k_j) / \langle \epsilon \rangle^{2/3}$  of turbulent and random fields, where  $\langle \epsilon \rangle$  is the mean energy dissipation rate per unit mass. Dotted lines: The corresponding spatial variability  $k_j^{5/3} [\tilde{E}^\ell(k_j) + \tilde{\sigma}^\ell(k_j)] / \langle \epsilon \rangle^{2/3}$ . Note that only one component of the vector field is plotted, i.e.,  $\ell=1$ , as all components are statistically equivalent due to isotropy.

The three velocity fields  $\mathbf{u}=(u^1, u^2, u^3)$ , sampled at resolution  $N=2048^3=2^{3J}$  (with  $J=11$  octaves), are decomposed into an orthogonal wavelet series using Coiflet 12 wavelets [13], such that

$$\mathbf{u}(\mathbf{x}) = \sum_{\lambda} \tilde{\mathbf{u}}_{\lambda} \psi_{\lambda}(\mathbf{x}), \quad (1)$$

where the multi-index  $\lambda=(j, \mathbf{i}, \mu)$  denotes, for each wavelet  $\psi_{\lambda}$ , the scale index  $j$  (varying from 0 to  $J-1$ ), the spatial index  $\mathbf{i}$  (having  $2^{3j}$  values for each  $j$  and  $\mu$ ), and the direction index  $\mu=1, \dots, 7$  [13,14]. Due to orthogonality, the wavelet coefficients are given by  $\tilde{\mathbf{u}}_{\lambda}=\langle \mathbf{u}, \psi_{\lambda} \rangle$ , where  $\langle \cdot, \cdot \rangle$  denotes the  $L^2$  inner product. The wavelet coefficients measure the fluctuations of  $\mathbf{u}$  at scale  $2^{-j}$  and around position  $\mathbf{i}/2^j$  for each of the seven possible directions  $\mu$ . The contribution of  $\mathbf{u}$  at scale  $2^{-j}$  is obtained by fixing  $j$  and summing only over  $\mathbf{i}$  and  $\mu$  in Eq. (1). By construction we have  $\mathbf{u}=\sum_j \mathbf{u}_j$ . From the scale-dependent kinetic energy, defined as  $\tilde{E}_j=\langle \mathbf{u}_j, \mathbf{u}_j \rangle/2$ , we obtain via scale orthogonality the total energy  $E=\sum_j \tilde{E}_j$ .

### III. NUMERICAL RESULTS

Relating scale  $2^{-j}$  with wave number  $k_j$  as  $k_j=k_{\psi}2^j$ , where  $k_{\psi}$  is the centroid wave number of the chosen wavelet ( $k_{\psi}=0.77$  for the Coiflet 12 used here), the wavelet energy spectrum for the  $\ell$ th component of velocity is defined as  $\tilde{E}^{\ell}(k_j)=\langle e_j^{\ell} \rangle/\Delta k_j$ , where  $e_j^{\ell}=(u_j^{\ell})^2/2$ ,  $\Delta k_j=(k_{j+1}-k_j)/\ln 2$ , and  $\langle \cdot \rangle$  denotes the spatial average. Note that  $\tilde{E}^{\ell}$  corresponds to a smoothed version of the Fourier energy spectrum [13,14]. For each velocity component, we can then quantify the spatial variability of the energy spectrum at a given wave number  $k_j$  as the standard deviation of  $\tilde{E}^{\ell}(k_j)$ , defined by

$$\tilde{\sigma}^{\ell}(k_j)=\sqrt{\langle (e_j^{\ell})^2 \rangle - \langle e_j^{\ell} \rangle^2/\Delta k_j}. \quad (2)$$

Figure 1 shows the compensated energy spectrum (i.e., the spectrum multiplied by  $k_j^{5/3}$ ) and the corresponding spatial variability for the three fields as a function of the dimensionless wave number  $k_j\eta$ , where  $\eta$  is the Kolmogorov dissipative scale [4]. By construction all fields have the same energy spectrum, however, the standard deviation of their spatial fluctuations  $\tilde{\sigma}^{\ell}(k_j)$  differs. The central wave number  $k_j$  is in the inertial subrange for  $j=3,4,5$ , where  $\tilde{E}^{\ell}(k_j) \propto k_j^{-5/3}$ , and we find that for scales  $j \geq 2$ , the spatial variability  $\tilde{\sigma}^{\ell}(k_j)$  is larger for the turbulent field (a) than for the two random fields.

To study higher order scale-dependent statistics we define the  $p$ th order centered moments of each component  $u^{\ell}$  of the vector field  $\mathbf{u}$  at scale  $2^{-j}$  by

$$M_p[u_j^{\ell}] = \langle (u_j^{\ell}(\mathbf{x}) - \langle u_j^{\ell}(\mathbf{x}) \rangle)^p \rangle. \quad (3)$$

For a relation between  $M_p[u_j^{\ell}]$  and the  $p$ th order velocity structure functions  $\zeta(p)$  we refer to [12]. The scale-dependent flatness of the velocity component  $u^{\ell}$ , defined as  $F[u_j^{\ell}]=M_4[u_j^{\ell}]/(M_2[u_j^{\ell}])^2$ , is related to the standard deviation of the spectral distribution of energy (2) by

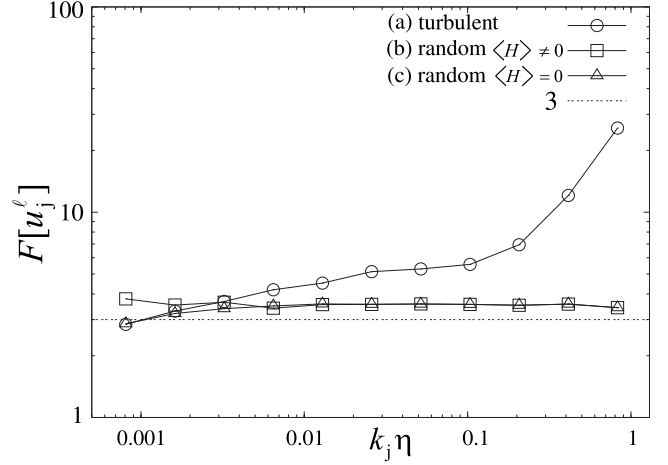


FIG. 2. Scale-dependent flatness  $F[u_j^{\ell}]$  of velocity for the turbulent (a) and for the two random fields (b) and (c).

$$F[u_j^{\ell}] = \left( \frac{\tilde{\sigma}^{\ell}(k_j)}{\tilde{E}^{\ell}(k_j)} \right)^2 + 1. \quad (4)$$

This demonstrates that the scale-dependent flatness  $F[u_j^{\ell}]$  based on the wavelet coefficients of velocity yields an easy way to compute a quantitative measure of the spatial variability of the energy spectrum [15].

To quantify the flow intermittency, we plot in Fig. 2 the scale-dependent flatness for the three different fields. We found that it increases with wave number for the turbulent field (a), while the two random fields have values that remain close to three at all scales, which is characteristic of Gaussian noise.

The PDFs of the corresponding vorticity fields  $\boldsymbol{\omega}=\nabla \times \mathbf{u}$  are presented in Fig. 3. For the two random fields the vorticity has a Gaussian PDF, while for the turbulent field it exhibits stretched exponential tails [16].

The flow helicity, defined as  $H=\mathbf{u} \cdot \boldsymbol{\omega}$ , gives a quantitative measure of the geometrical statistics of turbulence. The statistics of isotropic turbulence and their relevance to structures, e.g., large-scale flow and high dissipation regions,

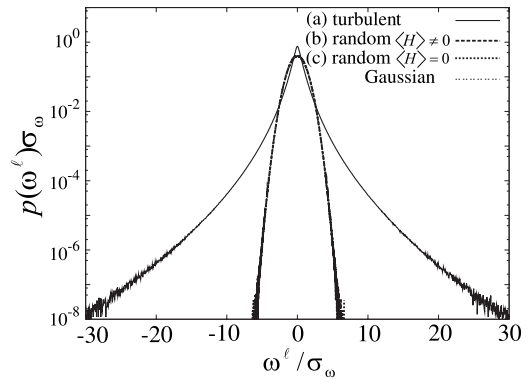


FIG. 3. PDF of vorticity for the turbulent field (a) and the two random fields (b) and (c), where  $\sigma_{\omega}$  is the standard deviation of the component  $\omega^{\ell}$ . Note that the PDFs of both random fields (b) and (c) perfectly superimpose with the Gaussian fit.

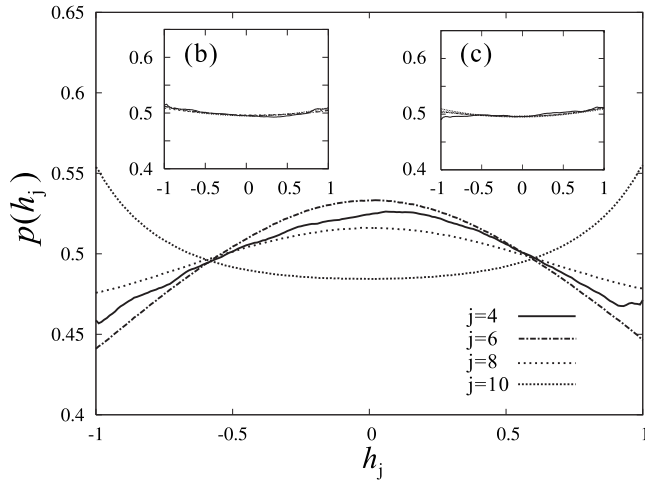


FIG. 4. PDFs of the relative helicity at different scales for the turbulent field (a). The insets (b) and (c) show the corresponding PDFs of the random fields (b) and (c), respectively.

have been examined since the late 1980s, for example, [17–19]. A review is beyond the scope of the paper; for further details we refer to [20,21]. We now introduce the scale-dependent helicity

$$H_j = \mathbf{u}_j \cdot \boldsymbol{\omega}_j, \quad (5)$$

where  $\mathbf{u}_j$  and  $\boldsymbol{\omega}_j$  are velocity and vorticity at scale  $2^{-j}$ , respectively. The scale-dependent helicity  $H_j$  ( $j \neq 0$ ) preserves Galilean invariance, though helicity  $H$  itself does not. The scale-dependent relative helicity is defined by  $h_j = H_j / (|\mathbf{u}_j| |\boldsymbol{\omega}_j|)$ . The evolution of its PDF with the scale is shown in Fig. 4 for the turbulent flow. The PDF of relative helicity presents a peak for  $h_j=0$  at scales  $j \leq 8$ , which corresponds to a higher probability for the vorticity and velocity vectors to be orthogonal, while at smaller scales  $j > 8$  it has two peaks at  $h_j = \pm 1$ , which correspond to a higher probability for vorticity and velocity vectors to be aligned or anti-aligned (Fig. 4). In contrast, the PDFs of the random fields (b) and (c) have almost constant values about 0.5 at all scales (Fig. 4, insets).

Figure 5 shows two-dimensional cuts of the modulus of vorticity at two different scales ( $j=4$  and  $j=8$ ), for the turbulent field (left) and for the helical random field (b) (right). We observe that the spottiness of the turbulent field increases when the scale decreases, which illustrates its intermittency. In contrast, the random field (b) exhibits a spatially homogeneous distribution whatever the scale, which confirms its nonintermittency. The same also holds for the random field (c) (not shown here).

To get further insight into the dynamics of Navier-Stokes turbulence, we analyze the Eulerian and Lagrangian accelerations defined as

$$\mathbf{a}_E = \frac{\partial \mathbf{u}}{\partial t} = -(\mathbf{u} \cdot \nabla) \mathbf{u} - \nabla P + \nu \nabla^2 \mathbf{u}, \quad (6)$$

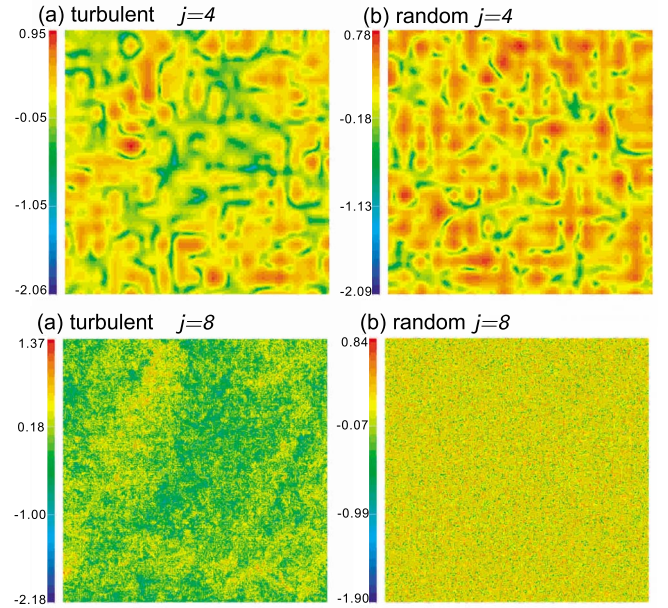


FIG. 5. (Color online) Two-dimensional cuts of the modulus of vorticity  $\log_{10}(|\boldsymbol{\omega}_j|/\sigma_j)$  at scales  $j=4$  and 8, where  $\sigma_j$  is the standard deviation of  $\boldsymbol{\omega}_j$ . Left: Turbulent field (a). Right: Helical random field (b). Only subdomains of half side length are shown.

$$\mathbf{a}_L = \frac{d\mathbf{u}}{dt} = -\nabla P + \nu \nabla^2 \mathbf{u}, \quad (7)$$

respectively, where  $P$  denotes the pressure,  $\nu$  is the kinematic viscosity, and where the density has been normalized to one. For a review on Lagrangian acceleration we refer to [22]. Using the PDF of  $\mathbf{a}_E$  and  $\mathbf{a}_L$  for the same data, it has already been found in [6] that the Lagrangian acceleration is more intermittent than the Eulerian acceleration. Here we focus on the scale-dependent PDFs and compare the turbulent field with the random fields. After decomposing both accelerations into an orthogonal wavelet series (1), we reconstruct their corresponding scale contributions  $\mathbf{a}_{E,j}$  and  $\mathbf{a}_{L,j}$ . In Figs. 6 and 7 we plot the PDFs of the Eulerian and Lagrangian accelerations at different scales for the turbulent field (a) and the random fields (b) and (c).

For the turbulent field the PDFs of both accelerations have stretched exponential tails, which become heavier at small scales. Furthermore, at each scale the Lagrangian acceleration exhibits heavier tails than the Eulerian one. This confirms that the former is more intermittent than the latter, in accordance with the conclusions drawn in [6] for the total PDFs.

For the random fields (b) and (c) the observations differ significantly. The PDFs of both Eulerian and Lagrangian accelerations have exponential tails, but without showing any scale dependence (insets in Figs. 6 and 7). The scale-dependent PDFs of the Eulerian acceleration are in good agreement with a Laplace distribution, which is not the case for the Lagrangian acceleration. This suggests that the term  $(\mathbf{u} \cdot \nabla) \mathbf{u}$ , which exhibits a Laplace distribution, is dominant in the Eulerian acceleration for all scales, as shown in [11]. We

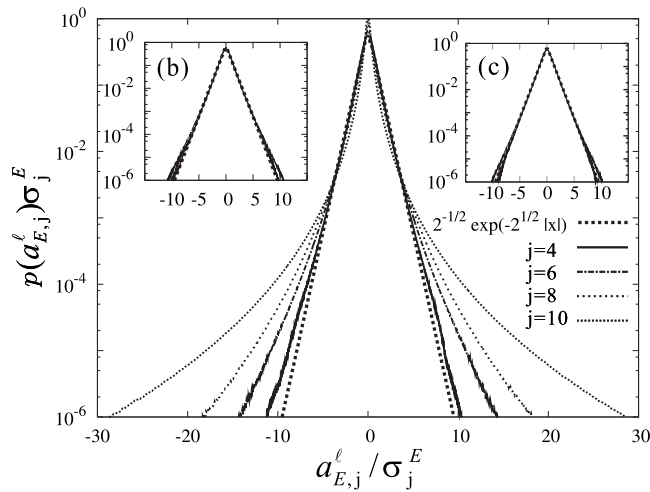


FIG. 6. Scale-dependent PDFs of the Eulerian acceleration for the turbulent field (a), where  $\sigma_j^E$  is the standard deviation of  $a_{E,j}^l$ . The insets show the corresponding PDFs for the random fields (b) and (c).

found that the flatnesses of both accelerations (Fig. 8) increase with scale for the turbulent flow, but the flatness of the Lagrangian acceleration is one order of magnitude larger than the flatness of the Eulerian acceleration, which shows the extreme intermittency of the former. In contrast, for both random flows the flatness remains almost constant, around 5 for the Lagrangian acceleration and around 6 for the Eulerian acceleration, which confirms that the latter yields a Laplace distribution (whose flatness is 6). This proves that the random fields are nonintermittent, as no scale dependence can be observed, even if their PDFs of acceleration are strongly non-Gaussian.

#### IV. CONCLUSIONS

The intermittency of the turbulent and random fields has been quantified using wavelet based scale-dependent statis-

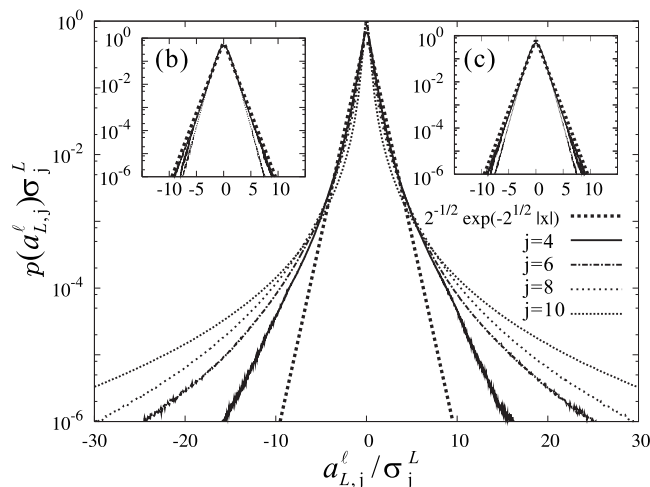


FIG. 7. Scale-dependent PDFs of the Lagrangian acceleration for the DNS field (a), where  $\sigma_j^L$  is the standard deviation of  $a_{L,j}^l$ . The insets show the corresponding PDFs for the random fields (b) and (c).

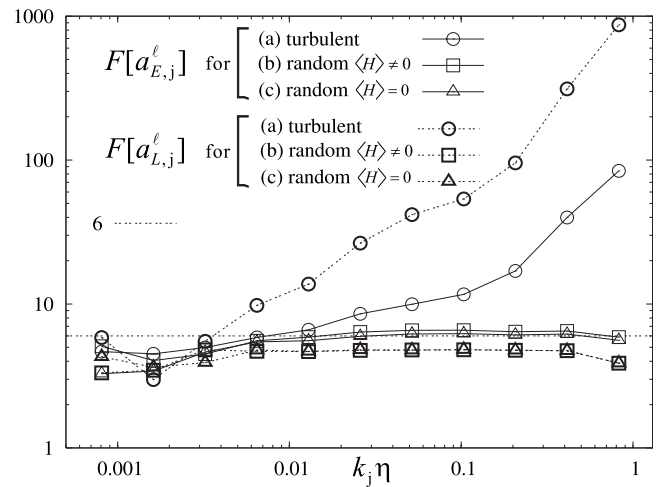


FIG. 8. Scale-dependent flatness of the Eulerian and Lagrangian accelerations for the turbulent field (a) and the random fields (b) and (c).

tics. It has been shown that the spatial variability of the energy spectrum is closely related to the scale-dependent flatness, which substantially increases for turbulence, while it remains constant at all scales for the random fields. A multi-scale measure to study geometrical statistics, the scale-dependent helicity, has been introduced. We found for the turbulent flow that the helicity and the PDFs of both Lagrangian and Eulerian accelerations strongly vary with scale, which is not the case for the random flows. These results confirm that scale-dependent statistics are necessary to characterize the intermittency of fully developed turbulent flows. An important consequence of this result is that divergence-free stochastic processes, having the same energy spectrum and velocity PDF as turbulent flows, cannot be used to model turbulent transport and mixing of scalars or particles, since, as long as they are nonintermittent, they do not preserve the scale behavior of acceleration. We also found that helicity does not play a statistically significant role for the random fields, as it does for turbulent flows. These results confirm the need for constructing intermittent stochastic processes to model turbulence, in a spirit similar to the advected delta-vee system [23], which could be done using the wavelet representation.

#### ACKNOWLEDGMENTS

The computations were carried out on the HPC2500 system at the Information Technology Center of Nagoya University. This work was supported by the Grants-in-Aid for the 21st Century COE “Frontiers of Computational Science,” and Scientific Research (B)20340099 from the Japan Society for the Promotion of Science (JSPS). M.F. and K.S. acknowledge financial support from the Agence Nationale de la Recherche, Project M2TFP, No. NT05-1-43391, and from the Association CEA/Euratom, contract No. V.3258.001. K.Y. is supported by a Grant-in-Aid for Young Scientists (B) 20760055 from the Ministry of Education, Culture, Sports, Science and Technology and JSPS. N.O. is grateful to the

Grant-in-Aid for JSPS fellows. The authors express their thanks to T. Ishihara, M. Yokokawa, K. Itakura, and A. Uno for providing us with the DNS data. We are grateful to R. Nguyen van Yen and Laurette Tuckerman for useful com-

ments. We thank the Isaac Newton Institute for Mathematical Sciences, Cambridge (U.K.), for hospitality and financial support during the program on “The Nature of High-Reynolds Number Turbulence.”

- 
- [1] U. Frisch, *Turbulence* (Cambridge University Press, Cambridge, England, 1995).
- [2] G. K. Batchelor and A. A. Townsend, Proc. R. Soc. London, Ser. A **199**, 238 (1949).
- [3] M. Yokokawa, K. Itakura, A. Uno, T. Ishihara, and Y. Kaneda, ACM/IEEE SC 2002 Conference, Baltimore (2002), p. 50.
- [4] Y. Kaneda, T. Ishihara, M. Yokokawa, K. Itakura, and A. Uno, Phys. Fluids **15**, L21 (2003).
- [5] Y. Kaneda and T. Ishihara, J. Turbul. **7**, 20 (2006).
- [6] T. Ishihara, Y. Kaneda, M. Yokokawa, K. Itakura, and A. Uno, J. Fluid Mech. **592**, 335 (2007).
- [7] F. Waleffe, Phys. Fluids A **4**, 350 (1992).
- [8] H. Chen, J. R. Herring, R. M. Kerr, and R. H. Kraichnan, Phys. Fluids A **1**, 1844 (1989).
- [9] Z. S. She, E. Jackson, and S. A. Orszag, Nature (London) **344**, 226 (1990).
- [10] M. Yamada and K. Ohkitani, Fluid Dyn. Res. **8**, 101 (1991).
- [11] T. Ishihara, Y. Kaneda, M. Yokokawa, K. Itakura, and A. Uno, J. Phys. Soc. Jpn. **72**, 983 (2003).
- [12] K. Schneider, M. Farge, and N. Kevlahan, in *Woods Hole Mathematics, Perspectives in Mathematics and Physics*, edited by N. Tongring and R. C. Penner (World Scientific, Singapore, 2004), Vol. 34, p. 302.
- [13] M. Farge, Annu. Rev. Fluid Mech. **24**, 395 (1992).
- [14] C. Meneveau, J. Fluid Mech. **232**, 469 (1991).
- [15] W. J. T. Bos, L. Liechtenstein, and K. Schneider, Phys. Rev. E **76**, 046310 (2007).
- [16] N. Okamoto, K. Yoshimatsu, K. Schneider, M. Farge, and Y. Kaneda, Phys. Fluids **19**, 115109 (2007).
- [17] R. B. Pelz, L. Shtilman, and A. Tsinober, Phys. Fluids **29**, 3506 (1986).
- [18] M. M. Rogers and P. Moin, Phys. Fluids **30**, 2662 (1987).
- [19] R. M. Kerr, Phys. Rev. Lett. **59**, 783 (1987).
- [20] H. K. Moffatt and A. Tsinober, Annu. Rev. Fluid Mech. **24**, 281 (1992).
- [21] J. M. Wallace, Phys. Fluids (to be published).
- [22] F. Toschi and E. Bodenschatz, Annu. Rev. Fluid Mech. **41**, 375 (2009).
- [23] Y. Li and C. Meneveau, Phys. Rev. Lett. **95**, 164502 (2005).